Effect of water content on the thermal degradation of amorphous polyamide 6,6

A collective variable-driven hyperdynamics study

Arash, Behrouz; Thijsse, Barend J.; Pecenko, Alessandro; Simone, Angelo

Important note
To cite this publication, please use the final published version (if applicable).
Please check the document version above.

Effect of water content on the thermal degradation of amorphous polyamide 6,6: A collective variable-driven hyperdynamics study

Behrouz Arash[a],[*], Barend J. Thijsse[c], Alessandro Pecenko[d], Angelo Simone[a],[b]

[a] Faculty of Civil Engineering and Geosciences, Delft University of Technology, Delft, The Netherlands
[b] Department of Industrial Engineering, University of Padova, Padua, Italy
[c] Department of Materials Science and Engineering, Delft University of Technology, Delft, The Netherlands
[d] Bosch Thermotechnik GmbH, Engineering New Technologies, Wernau, Germany

ARTICLE INFO

ABSTRACT

Thermal degradation under wet conditions is considered as an important aging mechanism in polyamide 6,6 (PA 6,6). The effect of water on thermal degradation of amorphous PA 6,6 is investigated at relatively low temperatures, varying from 1000 to 2000 K, using reactive force field molecular dynamics (MD) and collective variable-driven hyperdynamics simulations. The simulation of the related long-term chemical reactions is made possible thanks to the self-learning accelerated MD concept of hyperdynamics in combination with the corresponding accurate reproduction of the correct dynamics, consistent with unbiased MD simulations. The kinetics of cleavage reactions of the amide bonds in the backbone of the polymer chains, responsible for the thermal degradation of the polymer, is studied, and the influence of water content on the activation energy and pre-exponential factor of the cleavage reactions is explored. The results show that activation energy and pre-exponential factor are in agreement with experimental data. The proposed simulation framework not only estimates kinetic properties of thermal degradation that are consistent with experimental observations but also provides a predictive tool for studying long-term thermal degradation of PA 6,6.

1. Introduction

Thermal degradation of polymers is an aging process initiated at the molecular level under the influence of environmental factors such as high temperature and water. To gain insight into the physics of this degradation mechanism, atomistic simulations have been shown to be effective tools. Here, we perform atomistic simulations to characterize the effect of water on thermal degradation of polyamide 6,6 (PA 6,6).

PAs are commonly used in engineering applications due to their excellent thermal stability, high chemical resistance and cost-effective processing techniques [1,2]. They have proven to be particularly suitable as base resin for thermoplastic components that are expected to attain a long lifetime (several years) in contact with hot water. A typical example is the hydraulic circuit inside modern domestic water boilers, where PA-based polymer materials, among others, have replaced brass. As part failure is essentially caused by the material degradation induced by prolonged contact with an aggressive medium over time, understanding the mechanisms that initiate and propagate damage is the first necessary step towards a consistent prediction of failure [3,4].

Up to now, several experimental studies on thermal degradation of

PAs have been reported in the literature [5–12]. In these studies, some important factors affecting the mechanism of thermal degradation of PAs, such as temperature, additives, and polymer structures, were investigated. However, due to the complex physical scenario and the inherently limited resolution of experimental investigations, current techniques based on testing and past experience cannot provide sufficient physical insight that is essential to fully understand polymer degradation mechanisms. Another major drawback of the experimental investigations is the long time (up to several years) required to perform the tests [11,12] and the difficulty of isolating the influence of each parameter.

The development of numerical procedures based on atomistic simulation methods is therefore indispensable to explore degradation processes. In principle, simulation methods based on quantum mechanics (QM) enable to observe chemical reactions at the atomic level with accurate transition states [13] and can elucidate the mechanisms of polymer degradation. However, because of the high computational costs, QM simulations are only limited to small atomistic systems up to hundred atoms. Such small atomistic systems cannot represent the material behavior of bulk polymer systems. Molecular dynamics (MD)

simulations based on the reactive force field (ReaxFF) proposed by van Duin et al. [14], in contrast, allow the simulation of relatively large atomistic systems with an accurate description of the dissociation and formation of chemical bonds. ReaxFF is based on a bond order/bond distance relationship that allows a smooth transition from nonbonded to bonded systems. ReaxFF MD simulations trade off acceptable accuracy for a lower computational cost compared with QM simulations, making it possible to reach large enough time and size scales, nanoseconds and nanometers, respectively, for the study of polymer degradation.

ReaxFF has been used to simulate thermal degradation of various polymer materials [15–19]. Chenoweth et al. [15] extended ReaxFF using QM data to describe thermal decomposition of poly (dimethylsiloxane) (PDMS) polymer. The force field was then used to study non-isothermal degradation of the polymer at temperatures in the range 2400–3500 K with heating rates ($\geq 55 \times 10^{12}$ K/s) that can be considered unrealistic. To investigate the effect of pressure on the degradation process, the simulations were performed with densities varying from 0.973 g/cc (room temperature density) to a high density of 1.753 g/cc. Based on the rate of production of methane, the activation energy of PDMS decomposition was determined to be around 220 kJ/mol, without any verification against experimental data. The authors investigated the effect of various additives, including water, ozone and nitrogen monoxide, on thermal degradation of PDMS, and it was reported that the addition of reactive species leads to a significantly lower decomposition temperature; however, the effect of additives on the activation energy was not studied [16]. studied isothermal and non-isothermal degradation of epoxy resin using 25 ps ReaxFF MD simulations at high temperature (from 2300 to 4300 K) and high heating rates in the range $100 - 500 \times 10^{12}$ K/s. The evolution of small molecular products was determined, and it was shown that the dominant reaction pathways of epoxy resin degradation predicted by ReaxFF simulations are in agreement with those observed in experiments. However, the activation energy of the degradation was not compared with experimental data. ReaxFF MD was used in Ref. [17] to simulate isothermal degradation of high density polyethylene. Reaction mechanisms and generation pathways of gas products were obtained by 250 ps simulations at high temperature (from 2000 to 3000 K). The volatile products were assumed to be molecules with less than 31 carbon atoms. A kinetic model was obtained, and the activation energy, calculated from the evolution of the components, was determined to be around 250 kJ/mol, a value greater than the experimental results that are around 190 kJ/mol [20]. The difference may be mainly due to the high simulation temperatures and short simulation time, which would substantially affect the reaction mechanisms. Lu et al. [18] conducted a series of ReaxFF simulations over a timescale of 100 ps to study the pyrolysis mechanisms of polyimide (PI) at high temperatures ranging from 2800 to 3800 K. It was shown that the dominant products of PI pyrolysis are CO2 and CN. The time evolution profiles of the products were then used to obtain the kinetic properties of PI pyrolysis. The activation energy of PI pyrolysis was calculated to be 187 kJ/mol. It was shown that the activation energy obtained from ReaxFF simulations underestimates experimental values (201–274 kJ/mol). Most likely, this difference is the result of the high simulation temperatures.

These simulation studies have in common unrealistically high simulation temperatures (above 2000 K), and very short simulation time scales (below 250 ps). These limitations cause large uncertainties in the reaction mechanisms involved in thermal degradation of polymers and result in inaccurate predictions of the kinetic properties of the degradation processes. Furthermore, those degradation analyses of polymers are mainly based on the evolution of small volatile molecular compounds. Hence, the kinetics of cleavages in the backbone of polymer chains, responsible for degradation of the bulk material properties, and the influence of additives on the dissociation processes have remained poorly understood.

To address these issues, we investigate the mechanism of thermal

degradation of amorphous PA 6,6 using ReaxFF MD and collective variable-driven hyperdynamics (CVHD) simulations. The self-learning accelerated molecular dynamics concept of this hyperdynamics method allows simulations of long-time degradation reactions up to 0.17 μs at relatively low temperatures (down to 1000 K). Meanwhile, degradation analyses are conducted with unbiased MD simulations at high temperatures to verify that the dynamics produced by CVHD is correct. This combined scheme of unbiased MD and CVHD simulations therefore promises to improve the estimation of the kinetic properties of thermal degradation. The kinetics of cleavage of amide bonds in the backbone of the PA 6,6 chains, governing the evolution of thermal degradation in the polymer systems, is studied in Section 2 and further discussed in Section 3, where the effect of temperature and water concentration on the degradation rate is explored. The results show that both activation energy and pre-exponential factor predicted by the atomistic methods are consistent with the experimental data.

Our findings offer an in-depth insight into long-term thermal degradation processes in PA 6,6. Beyond this, the present study may have a broad impact on polymer degradation studies, in the sense that the proposed procedure can be extended to other types of polymers.

2. Methods

Simulations are performed to model the amorphous phase of PA 6,6, either dry or with 8 and 14 wt% water content. In practice the amount of water content in a PA 6,6 sample depends on adsorption time, temperature, its physical structure, and surrounding conditions (i.e., immersion in water or relative humidity), approaching 9 wt% in experiments [21]. Although the 14 wt% used in this study is somewhat too high, it allows a better assessment of the effect of water on thermal degradation in our simulations.

2.1. Molecular dynamics simulations

To study the chemical events associated with polymer degradation, we utilize the ReaxFF [14] force field as it fairly preserves the accuracy of quantum mechanics and enables MD simulations for modeling relatively large atomistic systems. In contrast to traditional force fields, ReaxFF allows simulation of chemical reactions accompanied with bond formation and breakage. The force field parameters used in this study are taken from Ref. [22] and are suitable for reactions with water. The construction of an amorphous PA 6,6 system is described next.

Firstly, a polymer chain with n= 20 monomers ($C_{12}H_{22}N_2O_2$) shown in Fig. 1, containing 40 amide groups and ethyl- and propyl-terminated, is built. The corresponding molecular weight (M_n) is around 4500 g/mol. An energy minimization is then performed using the conjugate-gradient method [23] to achieve a realistic three-dimensional model. Secondly, eight polymer chains are placed in a periodic $6.0 \times 6.0 \times 6.0$ nm^3 box with a predefined mass density of 0.25 g/cc. The total number of atoms is 6096. A geometry optimization with the convergence criterion of 0.0001 kcal/mol is performed to minimize the total energy of the system. Once the minimization process is completed, the system is allowed to equilibrate according to the constant volume and constant temperature ensemble (NVT) at 500 K for 50 ps. The simulation is followed by 30 ps in the isothermal-isobaric ensemble (NPT) at 1 bar and 500 K to equilibrate the density around 0.9 g/cc. The time step is set to be 0.25 fs and the Nosé-Hoover thermostat and barostat algorithms [24,25] are used for temperature and pressure control. Thirdly, water molecules are randomly placed in the
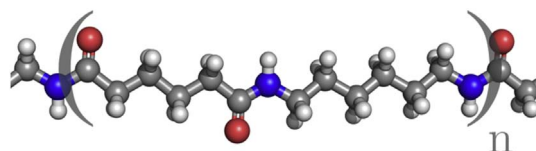
Fig. 1. Repeating unit of PA 6,6.

simulation box and the temperature of the system is decreased to 300 K at a cooling rate of 1 K/ps using a series of NVT simulations. Finally, an NPT simulation at 300 K and 1 bar is conducted for 1 ns, and configurations are extracted for the subsequent degradation analysis every 50 ps during the last 0.5 ns of the simulation. All simulations are performed with the Large-scale Atomic/Molecular Massively Parallel Simulator (LAMMPS) [26], and post-processing of the atomistic systems is done using OVITO [27].

2.2. Hyperdynamics simulations

MD simulations enable the study of the dynamical evolution of a general atomic system. However, they invariably suffer from severe time-scale limitations. This implies that unbiased MD simulations cannot be used beyond the nanosecond scale, while many relevant processes occur beyond the microsecond time-scale. To tackle this problem, we employ a CVHD method recently proposed by Ref. [28] to accelerate MD simulations. In hyperdynamics, simulations are not performed on the true potential energy surface $V(\mathbf{r})$, where $\mathbf{r}$ denotes the full collection of atomic coordinates, but on a modified potential $V^*(\mathbf{r})$ [29] that is obtained by adding the bias potential $\Delta V(\eta)$ to the original potential as in

$$V^*(\mathbf{r}) = V(\mathbf{r}) + \Delta V(\eta). \tag{1}$$

The bias potential is a function of a collective variable (CV) η, defined below, and is constructed, at time t, by summing Gaussian functions centered around the values of $\eta(t')$ at times preceding t according to

$$\Delta V(\eta) = \sum_{t'=\tau_G, 2\tau_G, \dots, t' < t} w \exp\left[-\frac{(\eta(t) - \eta(t'))^2}{2\delta^2}\right], \tag{2}$$

with width δ, height w, and deposition rate τ_G. The CV η is used in hyperdynamics to accelerate arbitrary processes in systems with many relevant degrees of freedom and is defined as [28]

$$\eta = \begin{cases} \frac{1}{2}(1 - \cos(\pi X_t^2)) & X_t \leq 1 \\ 1 & X_t > 1 \end{cases} \tag{3}$$

with the global distortion [30]

$$X_t = \left(\sum_{i=1}^{N} X_i^p\right)^{1/p}. \tag{4}$$

We use the exponent $p = 6$ in our calculations as recommended in Reference [28]. Here, the local distortions in Eq. (4) are calculated using bond length local properties

$$X_i = \begin{cases} 0 & r_i < r_i^{min} \\ \frac{r_i - r_i^{min}}{r_i^{max} - r_i^{min}} & r_i^{min} < r_i < r_i^{max}, \\ 1 & r_i > r_i^{max} \end{cases} \tag{5}$$

where r_i is the length of every bond, and r_i^{min} and r_i^{max} denote the begin and end lengths of reactive events, respectively. In the simulations, $r_i^{min} = 1.3\,\text{Å}$ and $r_i^{max} = 2.5\,\text{Å}$ are used for all carbon-nitrogen (C-N) bonds. Here, we use the nudged elastic band (NEB) method [31] to obtain information on the values of r_i^{min} and r_i^{max} associated with a transition state (i.e., the cleavage of C-N bonds). The variation of potential energy versus the C-N bond length in an amide group (CH$_3$CONH$_2$) calculated using the NEB method with 30 replicas of the system is presented in Fig. 2 from which $r_i^{min} = 1.3\,\text{Å}$ and $r_i^{max} = 2.5\,\text{Å}$. The dynamic biasing is applied to C-N bonds with Gaussian hill width $\delta = 0.05$, height hill $w = 1$ KJ/mol and deposition rate $\tau_G = 0.1$ ps. The width and height of the Gaussian functions used in the CVHD simulations are usual for bond-based CVs [28] with parameters optimized to obtain a good compromise between computational time and accuracy.

The average boost factor f (i.e., the acceleration compared with MD) is an ensemble average over the biased potential energy surface [29]
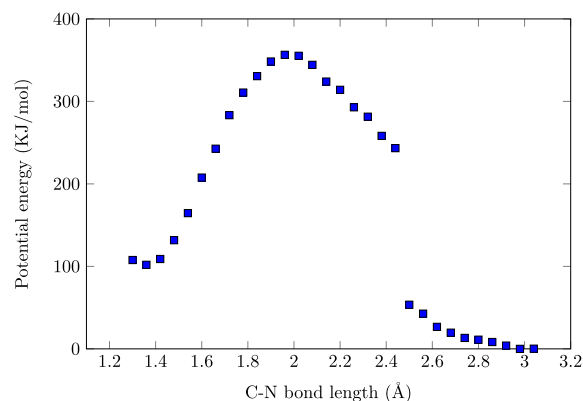
Fig. 2. Variation of potential energy versus the C-N bond length in an amide group obtained using the NEB method with 30 replicas of the system.

and is calculated as

$$f = \frac{t_{\text{hyper}}}{t_{\text{MD}}} = \langle e^{\beta \Delta V(\eta)} \rangle \tag{6}$$

with t_{hyper} the effectively simulated physical time or the hypertime, t_{MD} the MD time, and $\beta = 1/k_B T$ with the Boltzmann constant k_B.

2.3. Degradation analysis

Although different chain-scission mechanisms have been suggested in the literature for thermal degradation of polyamides, it is generally agreed that the chain scission most probably occurs either at the peptide C(O)-NH bonds or at the alkyl-amide $NH - CH_2$ bonds [32–34]. Therefore, the most frequent reaction pathway involved in degradation is the cleavage of C-N bonds in the backbone of the polymer chains due to the lower dissociation energy of C-N bonds (276 kJ/mol [32]) compared with the bond energy of C-C bonds (345 kJ/mol [32]). It is worth noting that the dissociation energies of C-N and C-C bonds obtained using the present ReaxFF are 255 and 318 kJ/mol, respectively.

To analyze the kinetics of the degradation process, a series of NVT simulations with a time step of 0.1 fs is performed on the equilibrated structure at high temperatures varying from 1000 to 2000 K. The NVT simulations are repeated ten times at each temperature. As mentioned earlier, the hyperdynamics method enables the simulation of long-term degradation reactions at lower temperatures compared with unbiased MD simulations. This significantly reduces uncertainties caused by elevated simulation temperatures in the degradation analysis. The physics behind the degradation process is as follows. Thermal degradation at high temperature leads to the breakage of bonds in the backbone of the polymer chains. Moreover, hydrolytic bond cleavage due to reactions between water molecules and polymer chains further accelerate the degradation process. To quantify the degree of degradation, the number of broken C-N bonds in the backbone of the polymer chains is calculated during the simulations, and the degree of degradation α is defined as the ratio of broken bonds (N_b) over the total number of C-N bonds (N_t):

$$\alpha = \frac{N_b}{N_t}. \tag{7}$$

The cleavage of bonds is defined using a bond order cutoff value equal to 0.3. The bond order is a threshold parameter defined in ReaxFF above which atoms are considered connected. The kinetic equation of the degradation reaction can be expressed as

$$\frac{d\alpha}{dt} = (1 - \alpha)k \tag{8}$$

where t, T, and k are simulation time, temperature, and the degradation rate, respectively. Under isothermal conditions, Eq. (8) can be

integrated to give

$$-\ln(1 - \alpha) = kt. \tag{9}$$

The temperature dependent degradation rate can be written using the Arrhenius equation as

$$\ln(k) = \ln(A) - \frac{E_a}{k_B}\frac{1}{T} \tag{10}$$

with A and E_a the pre-exponential factor and activation energy of degradation, respectively.

3. Results and discussion

In the following section, the mechanism of thermal degradation of amorphous PA 6,6 and the effect of water on the degradation process are first investigated using unbiased MD simulations at a high temperature. The kinetics properties of the polymer degradation are then studied, and the degradation rate k is measured at different water concentrations (c_w) using the first-order kinetics presented in Eq. (9). Next, we study the thermal degradation of amorphous PA 6,6 at relatively low temperatures, down to 1000 K, using the CVHD method. Finally, the activation energy and pre-exponential factor of the thermal degradation at different c_w are determined using the Arrhenius equation (10).

Fig. 4 presents the variation of the degree of degradation versus time for amorphous PA 6,6 depicted in Fig. 3. The simulation results are obtained by ten unbiased MD simulations at 2000 K and c_w= 0, 8 and 14 wt% with a standard deviation up to 5%. As shown in Fig. 4, the degree of degradation rapidly increases at the beginning and slows down with time. This observation can be interpreted by assuming that the concentration of unbroken C-N bonds is high at the beginning, resulting in a great probability of bond breaking. However, after a simulation time of around 12 ps, the low concentration of unbroken bonds induces a decrease in the rate of degradation. As expected, the degree of degradation increases in the presence of water compared with what is measured for dry polymer. For example, the degrees of degradation at c_w = 0 wt% (dry polymer) are around 0.28 and 0.50 after simulation time of 5 and 10 ps, respectively. The degrees of degradation respectively increase to 0.37 and 0.56 at c_w = 8 wt% and further raise to 0.45 and 0.60 by increasing c_w to 14 wt%. This implies that the presence of water accelerates the chemical reactions involved in the degradation process. This is in agreement with experimental observations that water content in polyamide accelerates the scission process of the polymer chains [11,35] by inducing hydrolysis. Fig. 5 shows the evolution of degradation versus time.

To investigate the degradation kinetics of PA 6,6, the former time
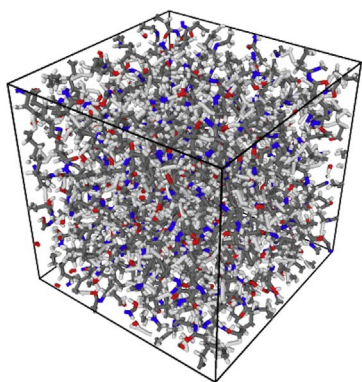
Fig. 3. Configuration snapshot of an equilibrated amorphous PA 6,6 system with eight chains of 20 monomers each and periodic boundary conditions. The colors of the atoms are as follows: gray for carbon, red for oxygen, blue for nitrogen, and white for hydrogen. (For interpretation of the references to colour in this figure legend, the reader is referred to the web version of this article.)
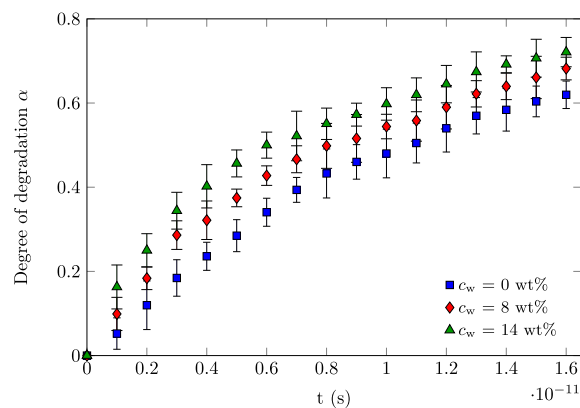
Fig. 4. Degree of degradation α versus time at 2000 K for c_w = 0, 8 and 14 wt% obtained by MD simulations. Each data point is the mean value of ten simulations; the error bars represent the standard deviation of uncertainty for each data point.

evolution profiles of the degree of degradation in Fig. 4, obtained from the mean values of ten simulations, are used to study the first-order kinetics of C-N bond breakage, described by Eq. (9), in Fig. 6. The degradation rate k at 2000 K and c_w = 0, 8 and 14 wt% is calculated with the aid of a linear fitting of the degree of degradation against the simulation time using a degree of degradation up to 0.6 in the fitting—this level of degradation assures that all polymer chains are broken into monomers or short oligomers. The results indicate that the rate of degradation is equal to 6.19×10^{11} s^{-1} at c_w = 0 wt% and increases to 7.35×10^{11} s^{-1} at c_w = 8 wt% and 8.95×10^{11} s^{-1} at c_w = 14 wt%. This further confirms that the water content in PA 6,6 accelerates its degradation process.

Next, we explore the kinetic properties of the degradation of amorphous PA 6,6 at temperatures that are significantly closer to the temperatures reported in experimental studies (600–800 K in Refs. [33,36,37]). Degradation analyses are therefore conducted using the hyperdynamics method that enables the simulation of long-term reactions. Fig. 7a and b show the time evolution of $\ln(1 - \alpha)$ at 1000 and 1400 K, respectively. From Fig. 7a, the degradation rate at 1000 K increases from 4.20×10^6 s^{-1} at c_w = 0 to 8.23×10^6 s^{-1} at c_w = 8 wt% and 1.27×10^7 s^{-1} at c_w = 14 wt%. The simulation results indicate an increase by a factor of 2 (3) in the degradation rate by increasing the water content in the polymer to 8 (14) wt%. A boost factor up to 200, corresponding to a time scale of 0.17 μs, is obtained in the hyperdynamics simulations at c_w = 0. As shown in Fig. 7b, the degradation rate at 1400 K and c_w equal to 0, 8 and 14 wt% are 3.20×10^9, 4.90×10^9 and 6.46×10^9 s^{-1}, respectively. A comparison between the degradation rates shows a substantial increase by three orders of magnitude in the degradation rate with increasing temperature from 1000 to 1400 K. This observation can be interpreted by considering that carbon and nitrogen atoms in the polymer chains have greater kinetic energy at higher temperatures to overcome the activation energy required for C-N bond breakage.

An estimation of the activation energy and the degradation rate k at a specific temperature can be obtained from the Arrhenius plot according to Eq. (10). To this end, the degradation rate at multiple temperatures varying from 1000 to 2000 K is calculated for c_w equal to 0, 8 and 14 wt%. The simulation data in this temperature range are obtained using MD and CVHD simulations with an overlap range between 1400 and 1500 K ($1/T$ between 6.67^{-4} and 7.14^{-4} K^{-1}). As shown in Fig. 8a and b, the data suggest a bilinear behavior rather than a simple linear fit corresponding to a single activation energy. Here, the fitting parameters are determined using the linear least square method; also the kink point ($1/T_k$) of the bilinear fit is determined by minimizing the least square error between the fit and the simulation data. A bilinear fit expresses a change of the activation energy at a certain temperature, and therefore possibly a change in the relaxation mechanism. At this point it is not fully understood what this change might be. A careful
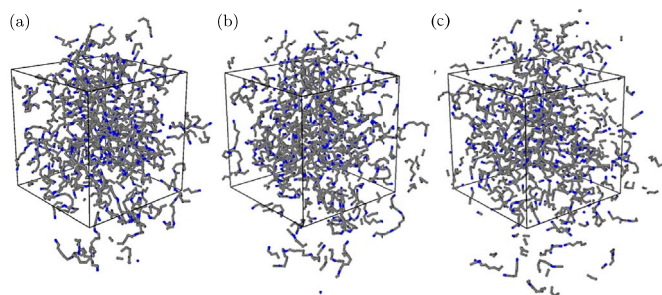
Fig. 5. Configuration snapshots of the evolution of degradation in the backbone of the polymer chains at 2000 K after (a) 5 ps, (b) 10 ps, and (c) 15 ps. The colors of atoms are as follows: gray for carbon and blue for nitrogen. Oxygen and hydrogen atoms are removed for the sake of clarity. (For interpretation of the references to colour in this figure legend, the reader is referred to the web version of this article.)
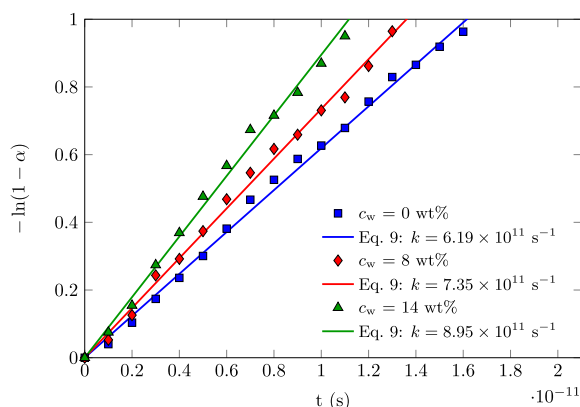
Fig. 6. Effect of c_w on the degradation rate (α) at 2000 K obtained with molecular dynamics.

Fig. 7. Effect of c_w on the degradation rate at (a) 1000 K, and (b) 1400 K obtained with hyperdynamics.

atomic-level analysis of the degradation events has not revealed a clear change in the microscopic reaction events. The fitting parameters of the Arrhenius plots in Fig. 8a and b are listed in Table 1 for the three water contents. In the following, we discuss the validity of the bilinear fit over this temperature range.

The results indicate a consistent decrease in the activation energy with increasing c_w for both fits. From the linear fit shown in Fig. 8a, the magnitude of the activation energy decreases from 160 to 156 to 154 kJ/mol by increasing c_w from 0 to 8 to 14 wt%, respectively. Similarly, from the bilinear fit in Fig. 8b, the activation energy at $1/T < 1/T_k$ (E_{a_1}) and $1/T > 1/T_k$ (E_{a_2}) decreases from 124 to 105 kJ/mol and from 201 to 193 kJ/mol by increasing c_w from 0 to 14 wt%. The reduction in the activation energy in the presence of water content in the polymer can be interpreted to mean that hydrolysis reactions between water molecules and amide compounds catalyze the breakage of C-N bonds, in turn providing an alternative path for the breakage reaction with a lower activation energy. Similar decreases in the activation energy have been reported in experimental studies [11,33] during PA 6,6 degradation. It can be seen that the activation energy and pre-exponential factor determined using the linear and bilinear fits at $c_w = 0$ are reasonably consistent with experimental data [33,38]. From Table 1 and for the bilinear fits, $1/T_k$ decreases from 7.58×10^{-4} to 7.22×10^{-4} K^{-1} with increasing c_w from 0 to 14 wt%. This implies that the kink point is outside the overlap range (i.e., 6.67×10^{-4} – 7.14×10^{-4} K^{-1}). From the present data it can be concluded that the transition point is not an artifact of the change of the simulation method but it is due to a real thermal effect. Furthermore, the root-mean-square error (RMSE) related to the bilinear fit (from 0.12 to 0.17 s^{-1}) is significantly lower than the that of the linear fit (from 0.41 to 0.48 s^{-1}). The RMSE of the bilinear fit also indicates that the overall fit errors are about equal to the differences between MD and CVHD data
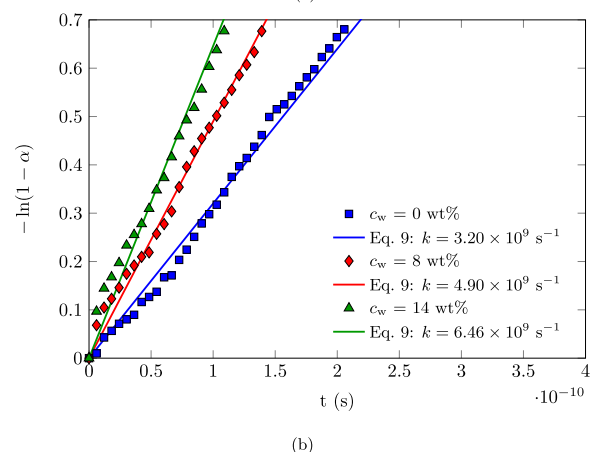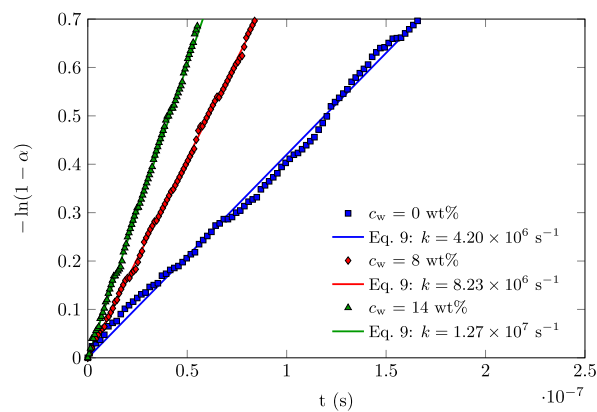
in the overlap range. This means that results obtained from MD and CVHD show no significant discrepancies. This analysis contributes to the credibility of the bilinear fit over the temperature range.

Furthermore, despite the fact that the temperature range 1000–2000 K used for the thermal degradation analysis is physically unrealistic, the accelerated MD concept of the CVHD method allows simulations of long-time degradation reactions at relatively low temperatures compared with unbiased MD simulations. This temperature range is much closer to those in experiments (i.e., 600–800 K [33,36,37]) and therefore significantly reduces uncertainties caused by too high simulation temperatures in unbiased MD simulations. In addition, this combined scheme of unbiased MD and hyperdynamics simulations allows us to verify that the dynamics produced by CVHD method is correct and promises to improve the estimation of the kinetic properties of thermal degradation. It is worth noting that extrapolation of the degradation rate using the Arrhenius plot to lower temperatures should be done with great care. Finally, the present combined scheme of unbiased MD and CVHD simulations can be equipped with reactive coarse-grained force fields [39–41] to allow the degradation analysis of polymer systems at larger length and time scales.

4. Summary and conclusions

ReaxFF MD and CVHD simulations have been used to investigate the thermal degradation of PA 6,6 at prescribed levels of water adsorption between 0 and 14 wt%. Based on the cleavage of C-N bonds in the backbone of the polymer chains, a kinetic model of thermal degradation has been obtained, where the effect of water uptake is included. Hyperdynamics has allowed to simulate relatively long-term degradation reactions over the time scale of 0.17 μs at temperatures between

(a)

(b)
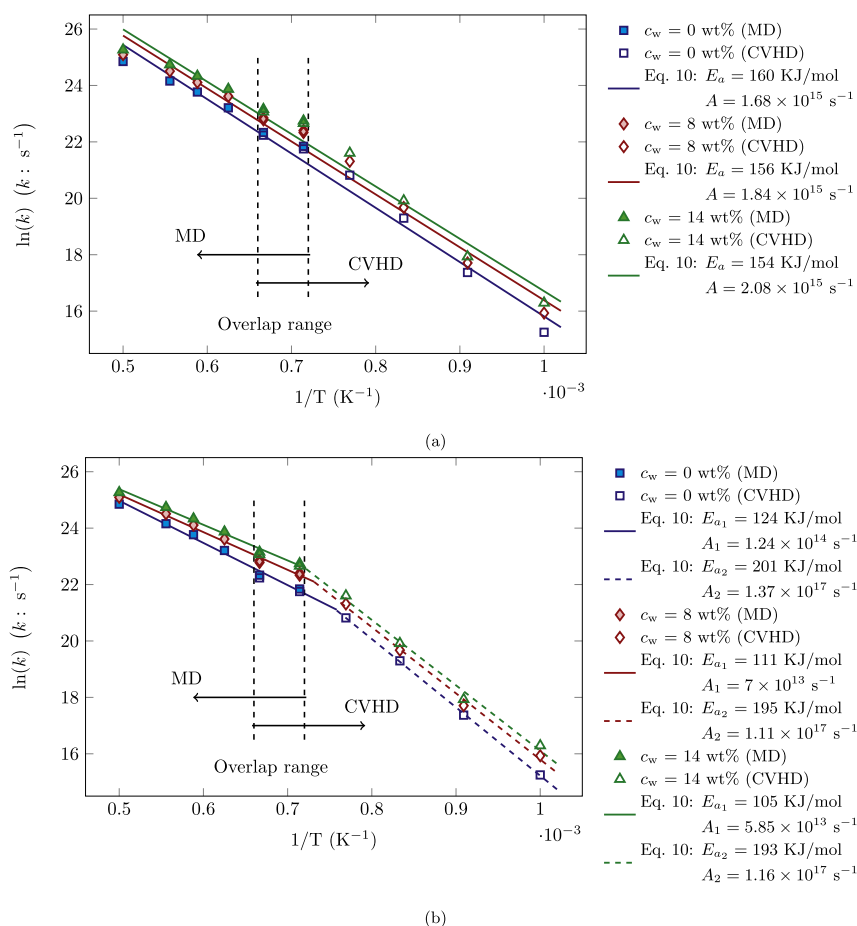
Fig. 8. Arrhenius plot of the degradation rate of PA 6,6. Natural logarithm of the degradation rate versus inverse temperature obtained by MD and CVHD simulations of PA66 at 1000–2000 K: (a) linear fit, and (b) bilinear fit.

Table 1
Parameters of the Arrhenius plots in Fig. 8a and b and those related to experiments. c_w, E_a, A and $1/T_k$ are water concentration in the polymer, the activation energy, the pre-exponential factor and the kink point, respectively.

		c_w (wt %)	0	8	14
Linear fit	E_a (KJ/mol)		160	156	154
	A (s^{-1})		1.68×10^{15}	1.84×10^{15}	2.08×10^{15}
	RMSE (s^{-1})		0.41	0.45	0.48
Bilinear fit	E_{a_1} (KJ/mol)		124	111	105
	A_1 (s^{-1})		1.24×10^{14}	7×10^{13}	5.85×10^{13}
	E_{a_2} (KJ/mol)		201	195	193
	A_2 (s^{-1})		1.37×10^{17}	1.11×10^{17}	1.16×10^{17}
	$1/T_k$ (K^{-1})		7.58×10^{-4}	7.31×10^{-4}	7.22×10^{-4}
	RMSE (s^{-1})		0.12	0.14	0.17
Experiments	E_a (KJ/mol)		130–225	–	–
	A (s^{-1})		$10^8 - 5 \times 10^{17}$	–	–

1000 and 2000 K, preserving the correct dynamics of the system. The major results of this study can be summarized as follows:

(1) the degradation rate increases by increasing temperature and water content –this observation is consistent with experimental reports in the literature [11,35];
(2) the activation energy of thermal degradation decreases by increasing the water content c_w in the polymer, while the pre-exponential factor increases with c_w; and

(3) the activation energy and pre-exponential factor for thermal degradation of dry PA 6,6 obtained from the ReaxFF simulations are in good agreement with experimental data [33,38].

It is worth noting that the CVHD method allows considerable freedom in the definition of local and global distortions in Eqs. (4) and (5). Nevertheless, a comparison between results obtained from MD and CVHD simulations for the kinetic properties of thermal degradation shows that the accuracy of the CVHD method does not suffer from this genericity.

Finally, the proposed simulation approach is, in principle, not restricted to short time intervals and high temperatures, which have been used in the present work to shorten the computational time, and can be employed to predict the isothermal and non-isothermal degradation of PA 6,6 in other aggressive media at significantly lower temperatures and heating rates compared with unbiased MD simulations.

References

[1] J. Lin, D.C. Sherrington, Recent developments in the synthesis, thermostability and liquid crystal properties of aromatic polyamides, Polymer Synthesis, Springer,

1994, pp. 177–219.

[2] F. Samperi, M.S. Montaudo, C. Puglisi, S. Di Giorgi, G. Montaudo, Structural characterization of copolyamides synthesized via the facile blending of polyamides, Macromolecules 37 (17) (2004) 6449–6459.

[3] H. Bockhorn, S. Donner, M. Gernsbeck, A. Hornung, U. Hornung, Pyrolysis of polyamide 6 under catalytic conditions and its application to reutilization of carpets, J. Anal. Appl. Pyrolysis 58 (2001) 79–94.

[4] L. Li, C. Guan, A. Zhang, D. Chen, Z. Qing, Thermal stabilities and the thermal degradation kinetics of polyimides, Polym. Degrad. Stab. 84 (3) (2004) 369–373.

[5] L. Peebles, M. Huffman, Thermal degradation of nylon 66, J. Polym. Sci. Part A-1 Polym. Chem. 9 (7) (1971) 1807–1822.

[6] A. Ballistreri, D. Garozzo, M. Giuffrida, P. Maravigna, G. Montaudo, Thermal decomposition processes in aliphatic-aromatic polyamides investigated by mass spectrometry, Macromolecules 19 (11) (1986) 2693–2699.

[7] B.J. Holland, J.N. Hay, Thermal degradation of nylon polymers, Polym. Int. 49 (9) (2000) 943–948.

[8] M. Schaffer, E. Marchildon, K. McAuley, M. Cunningham, Thermal nonoxidative degradation of nylon 6,6, J. Macromol. Sci. Part C Polym. Rev. 40 (4) (2000) 233–272.

[9] S. Jahromi, W. Gabriëlse, A. Braam, Effect of melamine polyphosphate on thermal degradation of polyamides: a combined X-ray diffraction and solid-state NMR study, Polymer 44 (1) (2003) 25–37.

[10] R. Shamey, K. Sinha, A review of degradation of nylon 6.6 as a result of exposure to environmental conditions, Rev. Prog. Coloration Relat. Top. 33 (1) (2003) 93–107.

[11] R. Bernstein, D.K. Derzon, K.T. Gillen, Nylon 6.6 accelerated aging studies: thermal–oxidative degradation and its interaction with hydrolysis, Polym. Degrad. Stab. 88 (3) (2005) 480–488.

[12] R. Bernstein, K. Gillen, Nylon 6.6 accelerating aging studies: II. Long-term thermal-oxidative and hydrolysis results, Polym. Degrad. Stab. 95 (9) (2010) 1471–1479.

[13] J. Gao, X. Wang, X. Li, X. Yu, H. Wang, Prediction of polyamide properties using quantum-chemical methods and BP artificial neural networks, J. Mol. Model. 12 (4) (2006) 513–520.

[14] A.C. Van Duin, S. Dasgupta, F. Lorant, W.A. Goddard III, ReaxFF: a reactive force field for hydrocarbons, J. Phys. Chem. A 105 (41) (2001) 9396–9409.

[15] K. Chenoweth, S. Cheung, A.C. Van Duin, W.A. Goddard, E.M. Kober, Simulations on the thermal decomposition of a poly (dimethylsiloxane) polymer using the ReaxFF reactive force field, J. Am. Chem. Soc. 127 (19) (2005) 7192–7202.

[16] Z. Diao, Y. Zhao, B. Chen, C. Duan, S. Song, ReaxFF reactive force field for molecular dynamics simulations of epoxy resin thermal decomposition with model compound, J. Anal. Appl. Pyrolysis 104 (2013) 618–624.

[17] X. Liu, X. Li, J. Liu, Z. Wang, B. Kong, X. Gong, X. Yang, W. Lin, L. Guo, Study of high density polyethylene (HDPE) pyrolysis with reactive molecular dynamics, Polym. Degrad. Stab. 104 (2014) 62–70.

[18] X. Lu, X. Wang, Q. Li, X. Huang, S. Han, G. Wang, A ReaxFF-based molecular dynamics study of the pyrolysis mechanism of polyimide, Polym. Degrad. Stab. 114 (2015) 72–80.

[19] A. Mlyniec, M. Ekiert, A. Morawska-Chochol, T. Uhl, Influence of density and environmental factors on decomposition kinetics of amorphous polylactide–Reactive molecular dynamics studies, J. Mol. Graph. Model. 67 (2016) 54–61.

[20] S. Kim, Y.-C. Kim, Using isothermal kinetic results to estimate the kinetic triplet of the pyrolysis of high density polyethylene, J. Anal. Appl. Pyrolysis 73 (1) (2005) 117–121.

[21] M. Paterson, J. White, Effect of water absorption on residual stresses in injection-moulded nylon 6,6, J. Mater. Sci. 27 (22) (1992) 6229–6240.

[22] O. Rahaman, A.C. van Duin, W.A. Goddard III, D.J. Doren, Development of a ReaxFF reactive force field for glycine and application to solvent effect and tautomerization, J. Phys. Chem. B 115 (2) (2010) 249–261.

[23] T.A. Straeter, On the Extension of the Davidon-broyden Class of Rank One, Quasi-newton Minimization Methods to an Infinite Dimensional Hilbert Space with Applications to Optimal Control Problems, Ph.D. thesis North Carolina State University, Raleigh, 1971.

[24] S. Nosé, A unified formulation of the constant temperature molecular dynamics methods, J. Chem. Phys. 81 (1) (1984) 511–519.

[25] W.G. Hoover, Canonical dynamics: equilibrium phase-space distributions, Phys. Rev. A 31 (3) (1985) 1695.

[26] S. Plimpton, Fast parallel algorithms for short-range molecular dynamics, J. Comput. Phys. 117 (1) (1995) 1–19.

[27] A. Stukowski, Visualization and analysis of atomistic simulation data with OVITO–the Open Visualization Tool, Model. Simul. Mater. Sci. Eng. 18 (1) (2009) 015012.

[28] K.M. Bal, E.C. Neyts, Merging metadynamics into hyperdynamics: accelerated molecular simulations reaching time scales from microseconds to seconds, J. Chem. Theory Comput. 11 (10) (2015) 4545–4554.

[29] A.F. Voter, Hyperdynamics: accelerated molecular dynamics of infrequent events, Phys. Rev. Lett. 78 (20) (1997) 3908.

[30] P. Tiwary, A. van de Walle, Accelerated molecular dynamics through stochastic iterations and collective variable based basin identification, Phys. Rev. B 87 (9) (2013) 094304.

[31] G. Henkelman, B.P. Uberuaga, H. Jónsson, A climbing image nudged elastic band method for finding saddle points and minimum energy paths, J. Chem. Phys. 113 (22) (2000) 9901–9904.

[32] B.G. Achhammer, F.W. Reinhart, G.M. Kline, Mechanism of the degradation of polyamides, J. Chem. Technol. Biotechnol. 1 (7) (1951) 301–320.

[33] S. Levchik, L. Costa, G. Camino, Effect of the fire-retardant ammonium polyphosphate on the thermal decomposition of aliphatic polyamides. Part III-Polyamides 6.6 and 6.10, Polym. Degrad. Stab. 43 (1) (1994) 43–54.

[34] S.V. Levchik, E.D. Weil, M. Lewin, Thermal decomposition of aliphatic nylons, Polym. Int. 48 (7) (1999) 532–557.

[35] N. Chaupart, G. Serpe, J. Verdu, Molecular weight distribution and mass changes during polyamide hydrolysis, Polymer 39 (6–7) (1998) 1375–1380.

[36] H. Qin, Q. Su, S. Zhang, B. Zhao, M. Yang, Thermal stability and flammability of polyamide 66/montmorillonite nanocomposites, Polymer 44 (24) (2003) 7533–7538.

[37] S. Jahromi, W. Gabriëlse, A. Braam, Effect of melamine polyphosphate on thermal degradation of polyamides: a combined X-ray diffraction and solid-state NMR study, Polymer 44 (1) (2003) 25–37.

[38] C. El-Mazry, M.B. Hassine, O. Correc, X. Colin, Thermal oxidation kinetics of additive free polyamide 6-6, Polym. Degrad. Stab. 98 (1) (2013) 22–36.

[39] K. Farah, H.A. Karimi-Varzaneh, F. Muller-Plathe, M.C. Bohm, Reactive molecular dynamics with material-specific coarse-grained potentials: growth of polystyrene chains from styrene monomers, J. Phys. Chem. B 114 (43) (2010) 13656–13666.

[40] B. Arash, H.S. Park, T. Rabczuk, Mechanical properties of carbon nanotube reinforced polymer nanocomposites: a coarse-grained model, Compos. Part B Eng. 80 (2015) 92–100.

[41] A.A. Mousavi, B. Arash, X. Zhuang, T. Rabczuk, A coarse-grained model for the elastic properties of cross linked short carbon nanotube/polymer composites, Compos. Part B Eng. 95 (2016) 404–411.